

# Spirooxazine- and spiropyran-doped hybrid organic–inorganic matrices with very fast photochromic responses

Barbara Schaudel,<sup>a</sup> Céline Guerneur,<sup>a</sup> Clément Sanchez,<sup>\*a</sup> Keitaro Nakatani<sup>b</sup> and Jacques A. Delaire<sup>b</sup>

<sup>a</sup>Laboratoire de Chimie de la Matière Condensée, URA CNRS 1466, Université Pierre et Marie Curie, 4 Place Jussieu, 75252 Paris, France

<sup>b</sup>Laboratoire de Photophysique et Photochimie Supramoléculaires et Macromoléculaires, URA CNRS 1906, ENS CACHAN, 61 Avenue du Président Wilson, 94235 Cachan Cedex, France

Both spirooxazine and spiropyran dyes have been embedded into two different hybrid matrices, which were formed from hydrolysis and cocondensation between diethoxydimethylsilane and zirconium propoxide and between methyldiethoxysilane (DH) and triethoxysilane (TH) respectively. The nature and the kinetics of the photochromic response depend strongly on the hydrophobic/hydrophilic balance (HHB) of the hybrid material. The HHB controls the competition between direct and reverse photochromism. The photochromic behaviour of the strongly hydrophobic spirooxazine-doped DH/TH coatings is direct, highly efficient ( $\Delta A > 1$ ), reversible and extremely fast (thermal bleaching time constant,  $k = 0.2 \text{ s}^{-1}$ ). The photochromic kinetics of this hybrid material are, to the best of our knowledge, much faster than those reported for spirooxazine in any other solid matrix.

The mild characteristics offered by the sol–gel process allow the introduction of organic molecules within an inorganic network.<sup>1</sup> Inorganic and organic components can then be mixed at the nanometric scale in virtually any ratio, leading to the so-called hybrid organic–inorganic nanocomposites.<sup>2–4</sup> These hybrids are extremely versatile in their composition, processing, and optical and mechanical properties.<sup>5</sup> Organic molecules play an important role in optics; many hybrid optical systems such as luminescent solar concentrators, solid-state dye lasers, optical sensors, photochromic and NLO devices have been developed in the past few years.<sup>6–9</sup>

Spiropyrans and spirooxazines are two of the fascinating families of molecules exhibiting photochromic properties. Upon irradiation, the colourless spiropyran or spirooxazine undergo a heterolytic C–O ring cleavage, producing coloured forms of merocyanines (Fig. 1). The merocyanines may interact with their environment, *i.e.* solvent, matrix *etc.*, leading to different photochromic responses. Levy and co-workers<sup>10,11</sup> first demonstrated the important role played by the dye–matrix interactions in the photochromic response of spiropyrans. They studied the photochromism of spiropyrans trapped in sol–gel matrices synthesized *via* polymerization of  $\text{Si}(\text{OCH}_3)_4$  or  $\text{RSi}(\text{OEt})_3$  ( $\text{R} = \text{ethyl, methyl, etc.}$ ) precursors, and observed two types of photochromic behaviour. When the photochromic dye is trapped within a hydrophilic domain of the matrix (domain containing residual Si–OH groups), the open zwitterionic coloured forms are probably stabilized through hydrogen bonding with the acidic silanol groups present at the pore surface. The result of this stabilization is the observation of the coloured forms before irradiation. These coloured forms can be bleached by irradiation in the visible range. This has been termed ‘reverse photochromism’. On the other hand, spiropyran dyes embedded in a more hydrophobic hybrid network made by hydrolysis of  $\text{RSi}(\text{OEt})_3$  exhibit direct photochromism, *i.e.* the colourless form is stable without irradiation. Such photochromic behaviour has been reported for many spiropyran- or spirooxazine-doped sol–gel matrices.<sup>12–17</sup> Moreover, for hybrid organic–inorganic matrices containing different chemical environments (hydrophilic and hydrophobic domains) a competition between direct and reverse photochromisms can be observed.<sup>17</sup> However, many fundamental questions still need to be considered. Little is known concerning the role of the photochromic dye–matrix

interactions on the kinetics of colouration and thermal fading. As far as photochromic devices are concerned, tuning between a strong and fast photochromic colouration (large  $\Delta A$ ) and a very fast thermal fading is needed. Usually spiropyran- or spirooxazine-doped sol–gel matrices or even spirooxazine-doped polymeric matrices exhibit slow thermal fading (at least several minutes).<sup>10–17</sup>

This article addresses the photochromic behaviour of a

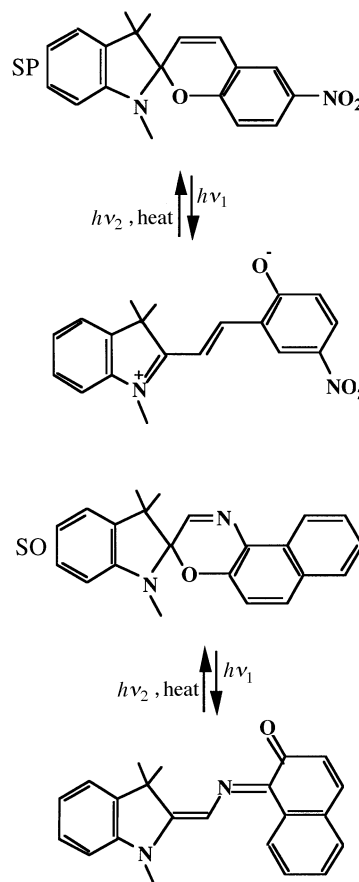


Fig. 1 Representation of the two photochromic dyes SP and SO and their open form

spiropyran, SP (6-nitro-1',3',3'-trimethylspiro-2*H*-1-benzopyran-2,2'-indoline) and a spirooxazine, SO [1,3,3-trimethylspiroindoline-2,3'-(3*H*)-naph(2,1-b)-(1,4)oxazine] (Fig. 1) embedded within two new hybrid matrices. The tuning of dye-matrix interactions allows us to obtain spirooxazine-doped hybrid coatings which exhibit a strong and very fast photochromic response.

Two kinds of hybrid matrices have been synthesized by using organically modified silicon alkoxide precursors  $[R'_xSi(OEt)_{4-x}]$  ( $R' = CH_3, H$ ), eventually cocondensed with zirconium alkoxide,  $Zr(OPr^n)_4$ .

## Experimental

### Synthesis

The SP and SO dyes were purchased from Aldrich.

The first SP- or SO-doped hybrid matrix was prepared as follows.  $(CH_3)_2Si(OC_2H_5)_2$  (D; Fluka), absolute ethanol and water in a  $y:0.5:y$  molar ratio were mixed for three minutes under magnetic stirring. The pH of the water was adjusted to 2 by addition of hydrochloric acid. The appropriate amounts of  $Zr(OPr^n)_4$  (Fluka) were added to the solutions in order to produce Zr:Si ( $x:y$ ) molar ratios ranging from 10:90 to 30:70. After ageing for 1 h, the photochromic dye solution ( $10^{-2}$  mol  $dm^{-3}$  in ethanol) was added to the sol. Samples will be labelled D/Zrx, where Zr stands for the zirconium,  $x$  for the amount of zirconium (Zr:Si,  $x:y$ ).

The second SP- or SO-doped matrix was prepared from the hydrolysis and cocondensation of  $(CH_3)HSi(OC_2H_5)_2$  (DH; ABCR) and  $HSi(OC_2H_5)_3$  (TH; Fluka), precursors. The DH:TH:EtOH:H<sub>2</sub>O (pH=7) molar ratios were 0.7:0.3:0.5:1. The dye solution ( $10^{-2}$  mol  $dm^{-3}$  in ethanol) was added after a few minutes. Samples are labelled DH70/TH30.

Bulk samples and coatings a few  $\mu m$  thick were prepared easily from both doped D/Zrx and DH70/TH30 sols.

### NMR experiments

The MAS NMR experiments were realised on a Bruker MSL 300 spectrometer using a Bruker 7 mm rotor. Spectra were recorded with 1  $\mu s$  pulses, a 0.1 s delay and a 5 kHz spinning speed for  $^{17}O$ , with 2  $\mu s$  pulses, a 10 s delay and a 4 kHz spinning speed for  $^{29}Si$  and with 3  $\mu s$  pulses, a 10 s delay and a 4 kHz spinning speed for  $^1H$  spectra. The positions of the NMR resonances were located taking  $Me_4Si$  ( $^{29}Si$  and  $^1H$ ) and water ( $^{17}O$ ) as  $\delta$  0 references.

The low natural abundance of the  $^{17}O$  nucleus [ $(3.7 \times 10^{-2})\%$ ] and its quadrupole moment renders its detection difficult. However, the use of 10%  $^{17}O$ -enriched water for the hydrolysis of precursors lead to a specific labelling of Si-O\*H, Si-O\*-Si and Si-O\*-M groups, and thus greatly enhances their detectability compared to ROH or Si-OR groups.

### FTIR spectroscopy

IR spectra were recorded on powdered samples with the conventional KBr pellet technique using a 550 Magna Nicolet FTIR spectrometer.

### Optical experiments

The photochromic behaviour of the samples was studied using the experimental setup described in Fig. 2. A xenon mercury arc lamp (450 W), providing light in the UV-VIS spectrum, was used to irradiate the sample. The appropriate irradiation wavelength was chosen by means of a narrow-band (10 nm) interference filter, and commutation of a shutter allowed us to make irradiation cycles. A beam from another light source, a xenon lamp (150 W), was used to follow the absorbance change

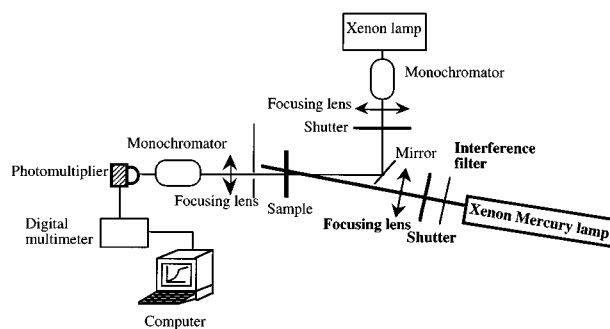


Fig. 2 Experimental setup used for photochromic behaviour studies

of the samples by measuring the light intensity transmitted through the sample during and after irradiation. The wavelength of this probe beam was selected by a set of two monochromators. Its intensity was attenuated strongly compared to the irradiation beam. The transmitted light was detected by a photomultiplier linked to a computer-driven digital multimeter (Keithley 2000). The incidence was close to normal for both beams.

Kinetics of bleaching were studied by following the fading of the absorbance ( $A$ ) at 490 nm for SP and 610 nm for SO, which are the absorption maxima in the visible region for the doped D/Zrx matrices. The thermal bleachings were fitted by using mono [ $A = B \exp(-kt) + C$ ] or bi-exponential [ $A = B \exp(-k_1t) + C \exp(-k_2t) + D$ ] equations.

## Results and Discussion

### Materials

The D/Zrx matrices have been characterized already by  $^{13}C$  MAS,  $^{29}Si$  MAS and CP MAS NMR studies.<sup>18,19</sup> These data revealed that these D/Zrx systems are hybrid nanocomposites made from polydimethylsiloxane chains and zirconium oxopolymers. Moreover, FTIR and DTA show that the zirconium oxopolymers are hydrophilic domains that still contain hydroxo groups coming from residual ethanol or Zr-OH ligands.<sup>20</sup> The size and the spacing between the  $ZrO_2$ -based domains is about a few nm, as indicated by SAXS.<sup>20</sup> However the nature of the interface between the PDMS chains and the zirconium oxo-based domains was not defined in these hybrid materials.  $^{17}O$  MAS NMR studies were therefore carried out to clarify the nature of the interface.

The  $^{17}O$  MAS NMR spectrum of the D/Zr20 matrix (Fig. 3) shows large resonances located at  $\delta$  400 and 290 which represent  $OZr_3$  and  $OZr_4$  respectively.<sup>21</sup> The assignment of the sharper resonance located at  $\delta$  336 is not obvious at the moment. It may be due to some residual molecular  $OZr_4$  species. The main peak at  $\delta$  73 is due to bridging  $OSi_2$  and the broad signal around  $\delta$  160 to Si-O-Zr bonds.<sup>22</sup> The

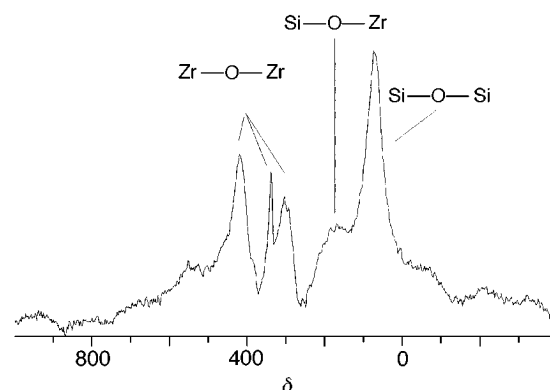


Fig. 3  $^{17}O$  MAS NMR spectrum of the D/Zr20 matrix

peaks assigned to homocondensation are then the major signals.

These data revealed clearly that these D/Zrx systems can be better described as a nanocomposite because homocondensation  $OZr_3$ ,  $OZr_4$ ,  $OSi_2$  species have been identified clearly. This composite is built from hydrophobic polydimethylsiloxane chains covalently linked through  $Zr-O-Si$  bonds to hydrophilic domains made of zirconium oxopolymers (Fig. 4).

The DH70/TH30 matrix was characterized by  $^1H$  MAS,  $^{29}Si$  MAS NMR and FTIR spectroscopies. The  $^{29}Si$  MAS NMR spectrum (Fig. 5) exhibited only two pairs of doublets located at  $\delta$  32.5, -36.8 and  $\delta$  82, -87.4. These resonances are due to fully condensed DH and TH units, respectively. The doublets are due to  $J$  coupling between Si and H via Si-H bonds. They are observed in the NMR solid-state spectrum because the  $^{29}Si$  resonances are particularly narrow suggesting a quasi-liquid behaviour of the DH and TH units. The ratio between these resonances is 70:30, as in the initial mixture, showing that upon hydrolysis and cocondensation reactions the Si-H bonds of DH and TH precursors have not been cleaved.<sup>24</sup>

The  $^1H$  MAS NMR spectrum (Fig. 6) exhibited one peak at  $\delta$  0.4 due to the methyl protons of the DH units and two peaks at  $\delta$  4.5 and 4.9 due to SiH in the TH and DH units respectively. The peaks at  $\delta$  1.4 and 4.0 which correspond to  $CH_3$  and  $CH_2$  groups, respectively, are due to residual species: ethoxy groups and a small proportion of ethanol. These species,

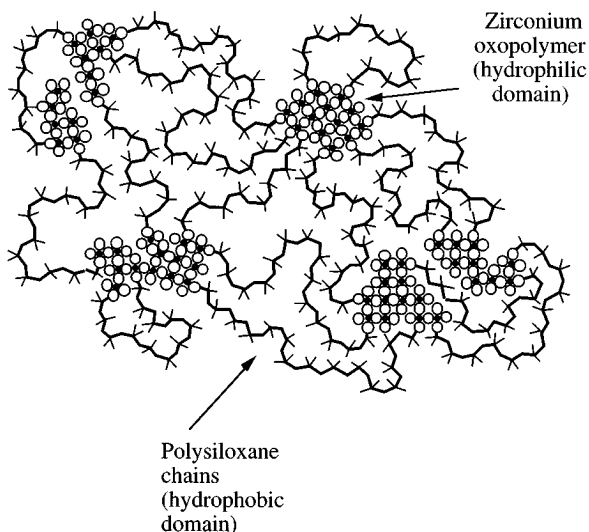


Fig. 4 Schematic representation of the D/Zr matrix

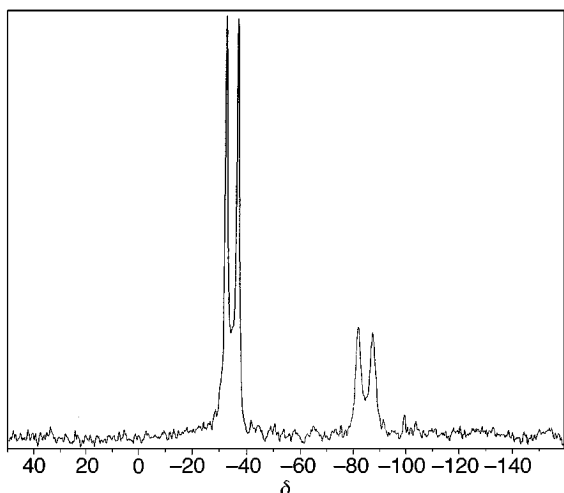


Fig. 5  $^{29}Si$  MAS NMR spectrum of the DH70/TH30 matrix

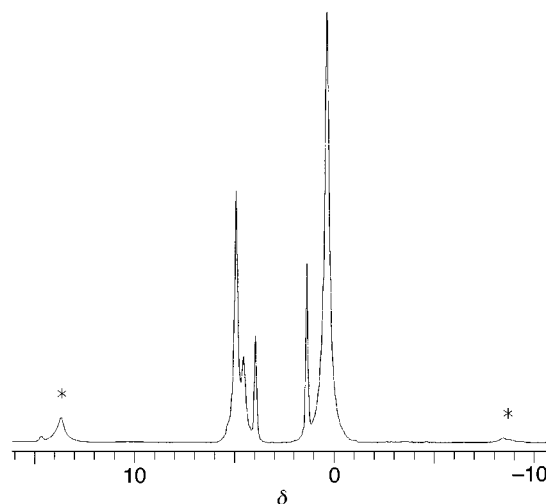


Fig. 6  $^1H$  MAS NMR spectrum of the DH70/TH30 matrix

according to the integration of the peaks, are in a 0.1:1 ratio with silicium. The network is then almost fully condensed.

In the FTIR spectrum of the DH70/TH30 coatings (Fig. 7) the presence of strong IR bands located at 2237 and 2176  $cm^{-1}$  confirmed that the Si-H bonds of the DH and TH precursors have not been cleaved. These bands correspond to  $\nu_{Si-H}$  in TH and DH units respectively. The DH70/TH30 coatings also exhibit strong IR bands located at 1000–1100  $cm^{-1}$ , indicating the formation of Si-O-Si linkages. Moreover, the 2300–4000  $cm^{-1}$  frequency range (the  $\nu_{O-H}$  region) is absolutely flat, suggesting that these matrices have an extremely low hydroxy group content. In agreement with data reported previously<sup>23</sup> the strongly hydrophobic DH/TH network can be described as a copolymer formed by short chains of DH units crosslinked by TH units.

Both D/Zrx and DH/TH exhibit glass-transition temperatures at about  $-100^\circ C$ <sup>23,24</sup> and their specific areas measured by nitrogen adsorption porosimetry are extremely low ( $< 5 m^2 g^{-1}$ ). These two matrices are very flexible and do not present any open porosity under nitrogen probing. At room temperature, both SP and SO dyes embedded in these hybrid matrices exhibit good stability. However, the photostability of these materials is currently under investigation.

#### Photochromic properties

D/Zrx matrices doped with SP or SO are lightly coloured (pink with SP or blue with SO) before irradiation. However, the absorbance in the visible region is weak in comparison with the total amount of embedded photochromic dyes. The amount of coloured form depends on  $x$ . Fig. 8 shows the photochromic behaviour of SP-doped D/Zrx gels for three  $x$

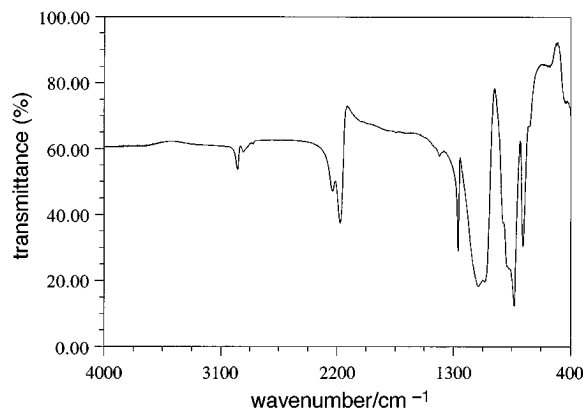
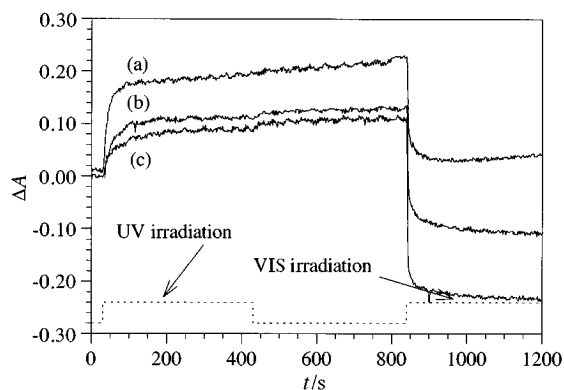


Fig. 7 IR spectrum of the DH70/TH30 matrix



**Fig. 8** Photocolouration ( $\lambda_{\text{irr}} = 320$  nm) and photodecolouration ( $\lambda_{\text{irr}} = 547$  nm) for SP-doped D/Zr bulks at 490 nm, (a) D/Zr10, (b) D/Zr20, (c) D/Zr30

values. When the amount of zirconium increases, the absorbance variation due to the colouration decreases while that due to decolouration increases: there are more open forms in the gel. The amount of coloured form increases proportionally with  $x$  and is much higher for D/Zr30 than for D/Zr10 samples.

This indicates that before irradiation the SO and SP dyes are split roughly into two populations. The coloured merocyanine open forms of SO and SP are stabilized by hydrogen bonding within the hydrophilic regions of the zirconium oxopolymers, while the closed SO and SP forms are probably located in the environment of the hydrophobic polydimethylsiloxane chains. Therefore, for these D/Zrx matrices the photochromism is partially reversible and can be balanced by tuning the D/Zr ratio.

The thermal bleaching behaviour of the D/Zr20 samples were fitted with a biexponential equation. The SP-doped materials exhibited a very long bleaching time (*ca.* 24 h) while for the SO-doped D/Zr20 materials the thermal fading was much faster. The rate constants for SO- and SP-doped D/Zr20 samples are reported in Table 1. For comparison, data from the literature concerning the photochromic properties of spiro-

pyran- and spirooxazine-doped sol-gel matrices and polymers are also given. The kinetic data of the SP- or SO-doped D/Zr20 samples are similar to those reported for other modified sol-gel matrices or in organic polymers.<sup>17,25</sup> As in organic polymers, the bleaching follows a biexponential equation which can be explained by an inhomogeneous distribution of free volumes in the gel. Moreover, the presence of different stereoisomers (*cis* or *trans*) could also account for this behaviour. The different isomer-matrix interactions could explain the different kinetics observed for SO and SP.

The thermal fading is longer for SP-doped hybrids than for SO-doped ones. This phenomenon can be correlated to the fact that SP open forms are known for their tendency to form zwitterionic species, while non-charged quinonic species are usually favoured for open SO molecules. Zwitterionic species can be stabilized markedly by hydrogen bonding with the matrix, thus lowering the decay times of thermal fading.

The SO or SP DH70/TH30 doped matrices exhibit normal photochromism. All the samples are colourless before irradiation. This is probably due to the strong hydrophobic character of this matrix. For the two photochromic dyes, the thermal fading can be fitted, with excellent agreement, to a monoexponential equation. This may be related to the quasi-liquid mobility observed by NMR for this matrix.

The rate constants obtained for the two dyes embedded in the DH70/TH30 matrix are also reported in Table 1. The thermal fading of SP in the DH70/TH30 matrix is faster than those reported for other sol-gel matrices<sup>10,11</sup> or for PMMA.<sup>25</sup>

The time dependence of the absorption upon repeated irradiation with 365 nm light for SO-doped DH70/TH30 coatings is reported in Fig. 9. The photochromic behaviour is reversible, extremely fast ( $k = 0.2 \text{ s}^{-1}$ ) and corresponds to a very high absorption jump ( $\Delta A = 1.2$ ). The photochromic kinetics of this SO-doped material are, to the best of our knowledge, much faster than those reported for SO in any other matrix (sol-gel matrices, organic polymers, alcohols, etc.).<sup>14,15,17,25,27</sup>

It is interesting to note that when embedded within the same DH70/TH30 matrix, SP shows a much longer thermal fading rate than SO. Moreover, a substantial part of the merocyanine form does not revert back to the initial form,

**Table 1** Photochromic behaviour of different spiropyrans and spirooxazines in sol-gel matrices, PMMA and ethanol (R=3-glycidoxypropyl, R'=3-aminopropyl)

chromophore	matrix	effect <sup>a</sup>	characteristics	ref.
SP	SiO <sub>2</sub>	D→R	D: $k = 6.7 \times 10^{-5} \text{ s}^{-1}$ R: $k = 1.7 \times 10^{-5} \text{ s}^{-1}$	10
	EtSiO <sub>1.5</sub>	D	$k = 1.7 \times 10^{-4} \text{ s}^{-1}$	11
	SiO <sub>2</sub> -Me <sub>2</sub> SiO	D→R	D: $k = 6.7 \times 10^{-5} \text{ s}^{-1}$ R: $k = 5 \times 10^{-5} \text{ s}^{-1}$	
	Me <sub>2</sub> SiO-ZrO <sub>2</sub>	D→R		this work
	MeHSiO-HSiO <sub>1.5</sub>	D	$k = 5 \times 10^{-3} \text{ s}^{-1}$	this work
	PMMA	D	$k_1 = 7 \times 10^{-4} \text{ s}^{-1}$ $k_2 = 10^{-4} \text{ s}^{-1}$	25
	ethanol	D	$k = 3.7 \times 10^{-4} \text{ s}^{-1}$	26
spiropyrans	SiO <sub>2</sub>	D/R	$t_{0.5} = 2.3 \times 10^5 \text{ s}$	
	MeSiO <sub>1.5</sub>	D		13
SO	MeSiO <sub>1.5</sub>	D	$k_1 = 1.15 \times 10^{-2} \text{ s}^{-1}$ $k_2 = 1.4 \times 10^{-3} \text{ s}^{-1}$	17
	RSiO <sub>1.5</sub> -EtSiO <sub>1.5</sub> -EtSiO <sub>1.5</sub>	D	$t_{0.5} = 2 \text{ s}$	14
	MeSiO <sub>1.5</sub> -RSiO <sub>1.5</sub> -R'SiO <sub>1.5</sub> -SiO <sub>2</sub> -Me <sub>2</sub> SiO	D	$t_{0.5} = 2 \text{ s}$	15
	Me <sub>2</sub> SiO-ZrO <sub>2</sub>	D→R	$k_1 = 3.1 \times 10^{-2} \text{ s}^{-1}$ $k_2 = 2 \times 10^{-3} \text{ s}^{-1}$	this work
	MeHSiO-HSiO <sub>1.5</sub>	D	$k = 0.2 \text{ s}^{-1}$	this work
	PMMA	D	$k_1 = 4 \times 10^{-2} \text{ s}^{-1}$ $k_2 = 4 \times 10^{-3} \text{ s}^{-1}$	25
	ethanol	D	$k = 0.2 \text{ s}^{-1}$	27
spirooxazine	SiO <sub>2</sub>	D/R	$k = 1.6 \times 10^{-3} \text{ s}^{-1}$	13
	MeSiO <sub>1.5</sub>	D	$k = 1.2 \times 10^{-2} \text{ s}^{-1}$	

<sup>a</sup>D, direct photochromism; R, reverse photochromism.

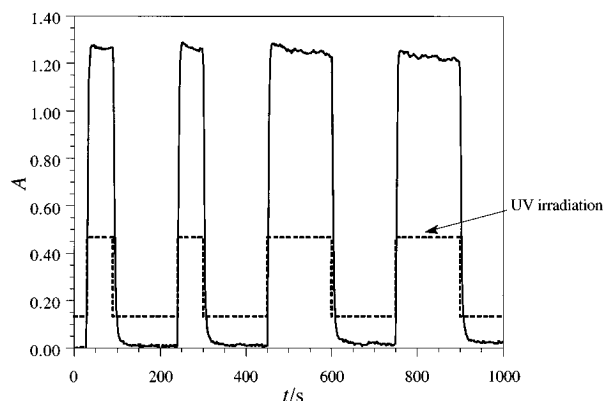


Fig. 9 Photocolouration ( $\lambda_{\text{irr}} = 365 \text{ nm}$ ) and thermal bleaching for the SO-doped DH70/TH30 film at 610 nm

even after two months. This phenomenon is probably due to the favoured zwitterionic form of the merocyanine SP which should interact slightly with the weakly polar  $\delta^+ \text{Si}-\text{H}^{\delta-}$  bonds<sup>28</sup> of the DH/TH matrix. As a consequence, the return of the SP dye to the closed form is slowed by these interactions.

## Conclusions

Photochromic hybrid materials were prepared by using SO and SP dyes in two different hybrid matrices (D/Zr and DH/TH). These experiments show the very high sensitivity of the photochromic behaviour of SO and SP dyes to dye-matrix interactions. The sol-gel materials, in particular the hybrid ones, allow tuning of these interactions, which are of paramount importance for control of the kinetics. The first matrix, D/Zr, shows reverse and direct photochromism. The ratio between reverse and direct photochromism increases with the amount of hydrophilic zirconium oxo polymers present in the material and emphasises that the open forms of these dyes are trapped *via* their interaction with residual M-OH groups. As in matrices presenting an inhomogeneous distribution of free volume, the photodynamics of these SO- and SP-doped D/Zr materials are not first order.

In contrast, the photodynamics of SO- and SP-doped hybrid matrices made from hydrolysis of methyldiethoxysilane and triethoxysilane (DH/TH) materials are first order, in agreement with the pseudo-liquid behaviour observed by solid-state NMR studies. SP dyes are very sensitive to weak dye-matrix interactions and are able to probe the weak polarity of Si-H bonds.

The negative partial charge carried by the hydrogen atoms of the Si-H bonds makes these DH/TH matrices strongly hydrophobic. This hydrophobicity is responsible for the direct and very fast photochromic behaviour observed. The SO-

doped DH/TH hybrid coatings exhibit, after a strong colouration ( $\Delta A > 1.2$ ) a very fast thermal bleaching, which is, to the best of our knowledge, the fastest thermal bleaching reported for spirooxazine-doped inorganic or organic materials.

## References

- 1 H. Schmidt and B. Seiferling, *Mater. Res. Soc. Symp. Proc.*, 1986, **73**, 739.
- 2 C. J. Brinker and G. Scherrer, *Sol-Gel Science, the Physics and Chemistry of Sol-Gel Processing*, Academic Press, San Diego, 1989.
- 3 B. M. Novak, *Adv. Mater.*, 1993, **5**, 422.
- 4 C. Sanchez and F. Ribot, *New J. Chem.*, 1994, **18**, 1007.
- 5 *Sol-Gel Optics, Processing and Applications*, ed. L. C. Klein, Kluwer Academic, Boston, 1993.
- 6 *Sol-Gel Optics I*, ed. J. D. Mackenzie and D. R. Ulrich, *Proc. SPIE*, vol. 1328, Washington, DC, 1990.
- 7 *Sol-Gel Optics II*, ed. J. D. Mackenzie, *Proc. SPIE*, vol. 1758, Washington, DC, 1992.
- 8 *Sol-Gel Optics III*, ed. J. D. Mackenzie, *Proc. SPIE*, vol. 2288, Washington, DC, 1994.
- 9 B. Dunn and J. I. Zink, *J. Mater. Chem.*, 1991, **1**, 903.
- 10 D. Levy and D. Avnir, *J. Phys. Chem.*, 1988, **92**, 734.
- 11 D. Levy, S. Einhorn and D. Avnir, *J. Non-Cryst. Solids*, 1989, **113**, 137.
- 12 D. Preston, J. C. Pouxviel, T. Novinson, W. C. Kaska, B. Dunn and J. I. Zink, *J. Phys. Chem.*, 1990, **94**, 4167.
- 13 H. Nakazumi, R. Nagashiro, S. Matsumoto and K. Isagawa, *SPIE Proc. Vol 2288, Sol-Gel Optics III, Proc. SPIE*, vol. 2288, San Diego, 1994.
- 14 L. Hou, B. Hoffmann, M. Menning and H. Schmidt, *J. Sol-Gel Sci. Technol.*, 1994, **2**, 635.
- 15 L. Hou, M. Menning and H. Schmidt, *J. Sol-Gel Sci. Technol.*, 1996, in press.
- 16 L. Hou, M. Menning and H. Schmidt, *Proc Eurogel'92*, 1992, 173.
- 17 J. Biteau, F. Chaput and J. P. Boilot, *J. Phys. Chem.*, 1996, **100**, 9024.
- 18 S. Diré, F. Babonneau, C. Sanchez and J. Livage, *J. Mater. Chem.*, 1992, **2**, 239.
- 19 S. Diré, F. Babonneau, G. Carturan and J. Livage, *J. Non-Cryst. Solids*, 1992, **147 & 148**, 62.
- 20 C. Guermeur and C. Sanchez, to be published.
- 21 T. J. Bastow, M. E. Smith and H. J. Whitfield, *J. Mater. Chem.*, 1992, **2**, 989.
- 22 F. Babonneau, J. Maquet and J. Livage, *Ceram. Trans.*, 1995, **55**, 53.
- 23 G. D. Soraru, G. D'Andrea, R. Campostrini and F. Babonneau, *J. Mater. Chem.*, 1995, **5**, 1363.
- 24 F. Babonneau, L. Bois, J. Livage and S. Diré, *Mater. Res. Soc. Symp. Proc.*, 1993, **286**, 289.
- 25 Y. Atassi, Thesis, Ecole Nationale Supérieure de Cachan France, 1996.
- 26 J. B. Flannery, *J. Chem. Soc. A*, 1968, 5660.
- 27 *Applied photochromic polymer systems*, ed. C. B. McArdle, New York, 1991.
- 28 A. P. Altshuller and L. Rosenblum, *J. Am. Chem. Soc.*, 1955, **77**, 272.

Paper 6/06859F; Received 7th October, 1996